

Preparation and Tribological Studies of Stearic Acid Self-Assembled Monolayers on Polymer-Coated Silicon Surface

Si-Li Ren,^{†,‡} Sheng-Rong Yang,^{*,†} Jin-Qing Wang,[†] Wei-Min Liu,[†] and Ya-Pu Zhao[‡]

State Key Laboratory of Solid Lubrication, Lanzhou Institute of Chemical Physics, Chinese Academy of Sciences, Lanzhou 730000, China, and State Key Laboratory of Nonlinear Mechanics, Institute of Mechanics, Chinese Academy of Sciences, Beijing 100080, China

Received July 2, 2003. Revised Manuscript Received October 9, 2003

We present a good alternative method to improve the tribological properties of polymer films by chemisorbing a long-chain monolayer on the functional polymer surface. Thus, a novel self-assembled monolayer is successfully prepared on a silicon substrate coated with amino-group-containing polyethyleneimine (PEI) by the chemical adsorption of stearic acid (STA) molecules. The formation and structure of the STA–PEI film are characterized by means of contact-angle measurement and ellipsometric thickness measurement, and of Fourier transformation infrared spectrometric and atomic force microscopic analyses. The micro- and macro-tribological properties of the STA–PEI film are investigated on an atomic force microscope (AFM) and a unidirectional tribometer, respectively. It has been found that the STA monolayer about 2.1-nm thick is produced on the PEI coating by the chemical reaction between the amino groups in the PEI and the carboxyl group in the STA molecules to form a covalent amide bond in the presence of *N,N*-dicyclohexylcarbodiimide (DCCD) as a dehydrating reagent. By introducing the STA monolayer, the hydrophilic PEI polymer surface becomes hydrophobic with a water contact angle to be about 105°. Study of the time dependence of the film formation shows that the adsorption of PEI is fast, whereas at least 24 h is needed to generate the saturated STA monolayer. Whereas the PEI coating has relatively high adhesion, friction, and poor anti-wear ability, the STA–PEI film possesses good adhesive resistance and high load-carrying capacity and anti-wear ability, which could be attributed to the chemical structure of the STA–PEI thin film. It is assumed that the hydrogen bonds between the molecules of the STA–PEI film act to stabilize the film and can be restored after breaking during sliding. Thus, the self-assembled STA–PEI thin film might find promising application in the lubrication of micro-electromechanical systems (MEMS).

1. Introduction

Micro-electromechanical systems (MEMS) are extremely miniaturized devices in which the frictional and adhesive forces dominate over inertial force and lead to damage to the smooth operation of the rotors or microgears due to the large surface-area-to-volume ratio.^{1–3} In resolving the friction-related problems, the ideal molecular lubricants for MEMS known as self-assembled monolayers (SAMs) have attracted much attention in recent years.^{4–6} The two most popular systems for this use are alkylthiols^{7–12} and alkyl-

silanes,^{13–21} which are produced on gold and silicon surfaces, respectively. Because silicon, polysilicon, silicon carbide, and other ceramic materials have been widely used as the materials to build MEMS devices,²²

* Corresponding author. E-mail: sryang@ns.lzb.ac.cn.

[†] State Key Laboratory of Solid Lubrication.

[‡] State Key Laboratory of Nonlinear Mechanics.

(1) Rymuza, Z. *Microsyst. Technol.* **1999**, *5*, 173.

(2) Zhao, Y. P.; Wang, L. S.; Yu, T. X. *J. Adhes. Sci. Technol.* **2003**, *17*, 519.

(3) Zhao, Y. P. *Acta Mechan. Sin.* **2003**, *19*, 1.

(4) Tsukruk, V. V. *Adv. Mater.* **2001**, *13*, 95.

(5) Ren, S.-L.; Yang, S.-R.; Zhang, J.-Y.; Zhang, X.-S. *Tribology* **2000**, *20*, 395 (in Chinese).

(6) Carpick, R. W.; Salmeron, M. *Chem. Rev.* **1997**, *97*, 1163.

(7) Laibinis, P. E.; Witesides, G. M.; Allara, D. L.; Tao, Y. T.; Parikh, A. P.; Nuzzo, R. G. *J. Am. Chem. Soc.* **1991**, *113*, 7152.

(8) Noy, A.; Frisbie, D. C.; Rozsnyai, L. F.; Wrighton, M. S.; Lieber, C. M. *J. Am. Chem. Soc.* **1995**, *117*, 7943.

(9) Touzov, I.; Gorman, C. B. *J. Phys. Chem. B* **1997**, *101*, 5263.

(10) Lee, S.; Shon, Y. S.; Lee, T. R.; Perry, S. S. *Thin Solid Films* **2000**, *358*, 152.

(11) Chen, S. F.; Li, L. Y.; Boozer, C. L.; Jiang, S. Y. *J. Phys. Chem. B* **2001**, *105*, 2975.

(12) Barrera, E.; Ocal, C.; Salmeron, M. *Surf. Sci.* **2001**, *482*, 1216.

(13) Maboudian, R.; Ashurst, W. R.; Carraro, C. *Sensors Actuators* **2000**, *82*, 219.

(14) Cha, K. H.; Kim, D. E. *Wear* **2001**, *251*, 1169.

(15) Gauthier, S.; Aimé, J. P.; Bouhacina, T.; Attias, A. J.; Desbat, B. *Langmuir* **1996**, *12*, 5126.

(16) Clear, S. C.; Nealey, P. F. *Langmuir* **2001**, *17*, 720.

(17) Bhushan, B.; Kulkarni, A. V.; Koinkar, V. N.; Boehm, M.; Odoni, L.; Martelet, C.; Belin, M. *Langmuir* **1995**, *11*, 3189.

(18) Bliznyuk, V. N.; Everson, M. P.; Tsukruk, V. V. *J. Tribology* **1998**, *120*, 489.

(19) Tsukruk, V. V.; Everson, M. P.; Lander, L. M.; Brittain, W. J. *Langmuir* **1996**, *12*, 3905.

(20) Srinivasan, U.; Houstonm, M. R.; Howe, R. T.; Maboudian, R. *J. Microelectromech. Syst.* **1998**, *7*, 252.

(21) Patton, S. T.; Cowan, W. D.; Eapen, K. C.; Zabinski, J. S. *Tribology Lett.* **2001**, *9*, 199.

(22) Spearing, S. M. *Acta Mater.* **2000**, *48*, 179.

studies of the SAMs derived from alkylsilanes have been extensively focused on resolving the tribological problems of MEMS.^{23–30}

Many micro-tribological studies indicate that SAMs with long hydrocarbon or fluorocarbon chains possess excellent lubrication and adhesive-resistant ability.^{18–20} However, the SAMs could be worn easily on a macroscale,^{14,21,23,31} as was reported on the ball-on-plate or pin-on-disk friction and wear behaviors of the SAMs of octadecyltrichlorosilane (OTS) (where the Hertzian contact stress usually ranges between 0.6 and 1.0 GPa, which is roughly consistent with that in the micro situation).^{14,23} In our previous study, a self-assembled dual-layer film was prepared by chemisorbing stearic acid molecules onto the SAMs of 3-(aminopropyl)-triethoxysilane to improve the anti-wear ability of SAMs.²⁴ A trilayer polymer film with hard–soft–hard nanoscale architecture was prepared by Tsukruk et al.³² They reported that, at modest loads, this coating showed a friction coefficient against hard steel below 0.06, which is lower than that for a classic molecular lubricant, alkylsilane SAMs; at the highest pressure (1.2 GPa) the sandwiched coating possessed four times higher wear resistance than the SAMs coating. An alternative approach to preparing film with good wear resistance is the formation of self-assembled films from dendrimers.^{33–37} Because of the multiple functional groups included in the dendrimers, these macromolecules are capable of forming a stable film via the multiple functional groups strongly attached to the substrate.⁴

Another kind of self-assembled multilayer film prepared by making use of the electrostatic layer-by-layer deposition technique was also extensively investigated.^{38–41} Huang et al. prepared self-assembled films of nitro-containing diazoresin and polysodium *p*-styrenesulfonate (NDR–PSS) and investigated their tribological behaviors. They found that the 10-bilayer film had better load-carrying and anti-wear abilities than the 1-bilayer film.⁴² Yu et al. reported that the tribo-

logical behaviors of the polyelectrolyte ultrathin multilayers were also closely related to the layer numbers.⁴³ However, few reports have been concerned with detailed and systematic tribological studies on this kind of multilayer. Because most of the polymers used to produce the layer-by-layer films contain strong polar groups, it is speculated that the resultant film surfaces will be hydrophilic. In other words, the film surfaces would possess high surface energy and hence increase the adhesion and friction of the multilayers, especially on a microscale. Such a shortcoming could be overcome by introducing a hydrophobic monolayer on the polymer-based film surface through physical or chemical derivatization. Garoff and his colleagues reported that the friction and adhesion of a cellulose surface was decreased sharply from a high level to a low level by physically impregnating a monolayer of fatty acids with long chains on the cellulose surface.⁴⁴ Though many efforts have been made on the chemical derivatization of functional polymer surfaces,^{45–51} few reports address the corresponding tribological studies. With this perspective in mind, we are engaged in the modification of polymer surfaces to improve their tribological properties in the present work.

2. Experimental Section

Materials. Polished single-crystal silicon (111) wafers (obtained from GRINM Semiconductor Materials Co., Ltd., Beijing) about 0.5-mm thick were used as the substrate. The aqueous solution of PEI (MW = 50 000–60 000) at a mass fraction of 50% was obtained from ACROS (New Jersey). Stearic acid (STA) and *N,N*-dicyclohexylcarbodiimide (DCCD) (Sheshan Chemical, Shanghai, China) were of analytical purity and used after purification. The solvent *n*-hexane (purity >98%) was used after dehydrating.

Preparation of the Stearic Acid Monolayer. Silicon wafers were cleaned and hydroxylated by immersing them in a piranha solution (a mixture of 7:3 (V/V) 98% H₂SO₄ and 30% H₂O₂) at 90 °C for 30 min. A thin layer of PEI was formed by immersing the silicon substrates into a dilute aqueous solution of PEI (0.2 wt %). After rinsing the PEI-coated substrates with ultrapure water and drying them in the N₂ flows, they were put into a dilute solution of STA and DCCD mixture in *n*-hexane (the initial concentrations of both STA and DCCD are 3 mM; precipitation is produced in the mixed solution in tens of min, so the solution is filtered before use). Finally, the samples were washed sequentially with *n*-hexane and acetone to remove the physisorbed impurities. Various immersion durations in the mixed solution were selected to investigate the adsorption kinetics of film formation. The experiments were carried out at room temperature.

Characterization of the Film. The static water contact angles on the films were measured with a Kyowa contact-angle

(23) Ren, S. L.; Yang, S. R.; Zhao, Y. P.; Zhou, J. F.; Xu, T.; Liu, W. M. *Tribology Lett.* **2002**, *13*, 233.

(24) Ren, S. L.; Yang, S. R.; Zhao, Y. P. *Langmuir* **2003**, *19*, 2763.

(25) Chandross, M.; Grest, G. S.; Stevens, M. J. *Langmuir* **2002**, *18*, 8392.

(26) Astrom, R.; Mutikainen, R.; Kuisma, H.; Hakola, A. H. *Wear* **2002**, *253*, 739.

(27) Zhang, L. Z.; Jiang, S. Y. *J. Chem. Phys.* **2002**, *117*, 1804.

(28) Zhang, L. Z.; Li, L. Y.; Chen, S. F.; Jiang, S. Y. *Langmuir* **2002**, *18*, 5448.

(29) Sugimura, H.; Ushiyama, K.; Hozumi, A.; Takai, O. *J. Vac. Sci. Technol. B* **2002**, *20*, 393.

(30) Hayashi, K.; Sugimura, H.; Takai, O. *Jpn. J. Appl. Phys.* **2001**, *40*, 4344.

(31) Rye, R. R.; Nelson, G. C.; Dugger, M. T. *Langmuir* **1997**, *13*, 2965.

(32) Sidorenko, A.; Ahn, H. S.; Kim, D. I.; Yang, H.; Tsukruk, V. V. *Wear* **2002**, *252*, 946.

(33) Tsukruk, V. V. *Adv. Mater.* **1998**, *10*, 253.

(34) Tsukruk, V. V.; Rinderspacher, F.; Bliznyuk, V. N. *Langmuir* **1997**, *13*, 2171.

(35) Zhang X. Y.; Wilhelm, M.; Klein, J.; Pfaadt, M.; Meijer, E. W. *Langmuir* **2000**, *16*, 3884.

(36) Zhang X. Y.; Klein, J.; Sheiko, S. S.; Muzafarov, A. M. *Langmuir* **2000**, *16*, 3893.

(37) Mueller, A.; Kowalewski, T.; Wooley, K. L. *Macromolecules* **1998**, *31*, 776.

(38) Decher, G.; Hong, J. D.; Schmitt, J. *Thin Solid Films* **1992**, *210–211*, 831.

(39) Lvov, Y.; Decher, G.; Mohwald, H. *Langmuir* **1993**, *9*, 481.

(40) Chen, J. C.; Huang, L.; Ying, L. M.; Luo, G. B.; Zhao, X. S.; Cao, W. X. *Langmuir* **1999**, *15*, 7208.

(41) Rubner, M. F.; Ferreira, M. *Macromolecules* **1995**, *28*, 7107.

(42) Huang, L.; Luo, G. B.; Zhao, X. S.; Chen, J. Y.; Cao, W. X. *J. Appl. Polym. Sci.* **2000**, *78*, 631.

(43) Gao, S.-Y.; Yu, L.-G. *Acta Polym. Sin.* **2003**, *1*, 18.

(44) Garoff, N.; Zauscher, S. *Langmuir* **2002**, *18*, 6921.

(45) Böhme, P.; Vedantham, G.; Przybycien, T.; Belfort, G. *Langmuir* **1999**, *15*, 5323.

(46) Popat, R. P.; Sutherland, I.; Sheng E. S. *J. Mater. Chem.* **1995**, *5*, 713.

(47) Chance, J. J.; Purdy, W. C. *Langmuir* **1997**, *13*, 4487.

(48) Sutherland, I.; Sheng, E.; Brewis, D. M.; Heath, R. J. *J. Mater. Chem.* **1994**, *4*, 683.

(49) Ameen, A. P.; Ward, R. J.; Short, R. D.; Beamson, G.; Briggs, D. *Polymer* **1993**, *34*, 1795.

(50) Chilkoti, A.; Ratner, B. D.; Briggs, D. *Chem. Mater.* **1991**, *3*, 51.

(51) Böhme, P.; Hicke, H. G.; Ulbricht, M.; Fuhrhop, J. H. *J. Appl. Polym. Sci.* **1995**, *55*, 1495.

meter. At least five replicate measurements were carried out for each specimen, and the measurement error was $\pm 1^\circ$.

The thickness of the films was measured on a Gaertner L116-E ellipsometer, which was equipped with a He-Ne laser (632.8 nm) set at an incident angle of 70° . A real refractive index of 1.46 was set for the silica layer and 1.45 was assumed for the PEI coating and STA monolayer. Five replicate measurements were carried out for each specimen and the thickness was recorded to an accuracy of 0.3 nm.

Fourier transformation infrared spectra were recorded on a Bruker IFS 66V/S. By using transmission mode, the spectrum was collected for 500 scans at a resolution of 4 cm^{-1} . To eliminate or decrease the interfering of H_2O and CO_2 , the sample chamber and optical chamber were vacuumed to 3 mbar. The freshly cleaned single-crystal silicon wafer was used as the reference.

A SPA400 (Seiko Instruments Inc.) atomic force microscope (AFM) was employed to observe the film morphology using tapping scanning mode.

The nano-tribological behaviors of the films were characterized with an AFM/FFM (friction force microscope) controlled by RHK electronics (RHK Technology, Rochester Hills, MI). Commercially available Si_3N_4 cantilevers/tips with a nominal force constant of 0.5 N/m and tip radius of less than 50 nm (Park Instruments, Sunnyvale, CA) were employed. To obtain the adhesive force between the AFM tip and the film surface, the force-distance curve was recorded and the pull-off force reckoned as the adhesive force. The frictional and adhesive forces of 4 and 10 replicate tests are averaged and reported in the present work. All the friction and adhesion tests were conducted at room temperature (about 21°C) and a relative humidity of 65%.

The macro-tribological behaviors of the films were evaluated on a DF-PM unidirectional tribometer. The lower specimen slides against an upper counterpart ball made of Si_3N_4 (ϕ 4 mm) with an rms roughness of about 8.6 nm, at a certain velocity and for a distance of 7 mm. Prior to the test, the ceramic ball was cleaned with acetone-soaked cotton. Loads of 0.5, 1, 2, and 3 N were selected, and the corresponding initial Hertzian contact stresses were estimated to be about 0.7, 0.9, 1.1, and 1.3 GPa, respectively. The friction coefficient and sliding cycles were recorded automatically. It was assumed that lubrication failure of the film occurred as the friction coefficient rose sharply to a higher value similar to that of a cleaned silicon wafer against the same counterpart (about 0.65). The sliding cycle at this point was recorded as the wear life of the film. All the tests were conducted at room temperature (25°C) and a relative humidity of 45%.

The morphologies of the worn surfaces were observed with a JSM-5600LV scanning electron microscope (SEM).

3. Results and Discussion

3.1 Formation and Characterization of the Films.

Branched polyethyleneimine {PEI, $-\text{[C}_2\text{H}_5\text{NHC}_2\text{H}_5\text{-N(C}_2\text{H}_5\text{NH}_2\text{)C}_2\text{H}_5\text{NH]}_n\text{-}$ }, with the ratio of primary, secondary, and tertiary amino groups of 1: 2: 1, can be easily adsorbed onto any hydroxylated solid surfaces through hydrogen bonds and van der Waals forces.^{47,52-55} Furthermore, the primary and secondary amino groups can be readily modified by carbonyl chloride, anhydride, and carboxylic acid. The PEI-coated silicon wafer was modified by generating a self-assembled monolayer of STA through chemical reaction between PEI and STA in the presence of DCCD as the dehydrating agent.

Scheme 1. Generation of an STA Monolayer on PEI-Coated Si Surface by Chemical Adsorption in the Presence of DCCD as a Dehydrating Agent in the Reacting Solution

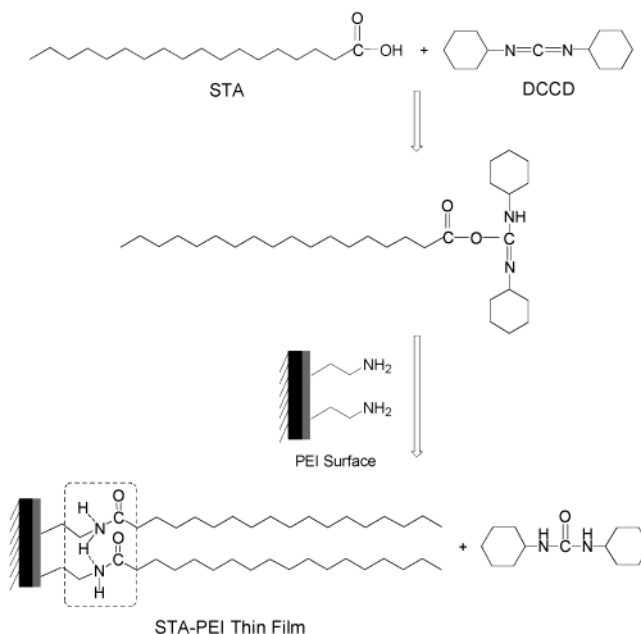


Table 1. Contact Angle and Thickness for the Silica Layer and the Organic Film Thereon

film	contact angle ($^\circ$)	thickness (nm)
SiO_2/Si	~ 0	1.9
PEI coating	9	0.7
STA monolayer	105 (56 ^a)	2.1 (0.4 ^a)

^a Represents the contact angle and thickness of the STA monolayer prepared in the absence of DCCD in the reacting solution.

The reaction process for STA molecules to chemisorb onto the PEI surface is shown in Scheme 1.

We first examine the variation of the contact angle on various surfaces, as it is sensitive to the surface chemical composition. The contact angles for water on the hydroxylated silicon surface and the self-assembled films thereon are shown in Table 1. It can be seen that the hydroxylated silicon surface and the PEI coating (obtained by immersing the substrate in the PEI aqueous solution for 15 min) have water contact angles about 0° and 9° , respectively, which indicates that both surfaces are hydrophilic. This is attributed to the hydroxyl groups distributed on the hydroxylated silicon surface and the amino-groups in the PEI coating. Once the STA layer is produced by immersing the PEI-coated wafer in the mixed solution of STA and DCCD for 24 h, the contact angle greatly increases to 105° and the resulting film surface becomes hydrophobic. We also examine the role of DCCD in the formation of STA monolayer on the PEI-coated Si substrate. From Table 1, we can see that the contact angle and thickness are only about 56° and 0.4 nm, respectively, for the same PEI-coated silicon substrate immersed in STA solution without DCCD for 24 h, which indicates that the STA monolayer in this case has poor quality. This is attributed to the fact that STA was only physically adsorbed onto the PEI-coated Si surface by way of hydrogen-bonding or electrostatic interaction in the absence of the DCCD, whereas DCCD as the dehydrat-

(52) Bahulekar, R.; Ayyangar, N. R.; Ponrathnam, S. *Enzyme Microb. Technol.* **1991**, *13*, 858.

(53) Gao, M.; Richter, B.; Stefan, K. *Adv. Mater.* **1997**, *9*, 802.

(54) Ren, S.-L.; Yang, S.-R.; Wang, J.-Q.; Qi, S.-K.; Zhao, Y.-P. *Acta Chim. Sinica* **2001**, *59*, 1894.

(55) Ren, S.-L.; Yang, S.-R.; Xue, Q.-J. *Acta Physico.-Chim. Sinica* **2001**, *17*, 97 (in Chinese).

Table 2. Effect of Real Refractive Index on the Measured Thickness of Polymer PEI Film

refractive index	thickness of sample 1 (nm)	thickness of sample 2 (nm)	thickness of sample 3 (nm)
1.40	0.72	0.90	0.81
1.45	0.67	0.86	0.72
1.50	0.60	0.76	0.73
1.55	0.58	0.75	0.67

ing reagent in the STA solution functions to enhance the chemical reaction between the amino groups in PEI and the carboxyl group in STA molecules, with the formation of covalent amide bonds (Scheme 1).⁵⁶

Formation of the chemical bonds between the STA and PEI implies that the STA might be monolayer thick. To confirm this, the film thickness was measured by ellipsometry and the results are listed in Table 1. After hydroxylation in the piranha solution at 90 °C for 30 min, a silica layer about 1.9 nm thick is generated on the silicon wafer. The PEI coating is about 0.7 nm thick, indicating that the polymer chains of the PEI monolayer are laterally arranged on the silicon surface. The STA monolayer is about 2.1 nm thick, which is a little bit smaller than the 2.6 nm measured for the STA-SAMs on Al,⁵⁷ reflecting that the STA monolayer is not packed densely enough and the STA molecules might be tilted on the PEI surface. This is attributed to a low density of the amino group on the PEI surface or to incomplete derivatization of the amino groups by the STA molecules. A real refractive index of 1.45 was used to measure the STA monolayer thickness, which is nearly equal to the datum of 1.47 used in the literature. To estimate the accuracy of the thickness measurement of the PEI film with respect to the refractive index 1.45, we made a series of measurements within the refractive index range from 1.40 to 1.55. The results are listed in Table 2. It can be seen that the thickness of the PEI film assumes minor decreases with increasing refractive index. Thus, the refractive index 1.45 used in the ellipsometric measurement could well reflect the actual thickness of the PEI film.

The adsorption kinetics of the PEI film on the Si substrate and of the STA on the PEI film was investigated by examining the variations of the film thickness and contact angle with the adsorbing duration. As shown in Figure 1a, the PEI film deposited at adsorption durations from 5 min to 10 h on the Si substrate shows almost the same thickness (0.6–0.8 nm), indicating that the PEI adsorption is fast and that extension of the adsorbing duration does not lead to generation of a thicker PEI layer. This is rationally understood considering that polymeric PEI, a kind of cationic polyelectrolyte containing abundant amino groups, can be easily protonized in water. On one hand, because of the electrostatic repulsion in the chain, the PEI molecule takes an extended and stiff conformation in its dilute aqueous solution and adopts a flat structure when it adsorbs onto the silicon surface. On the other hand, because of the electrostatic repulsion between the chains, the PEI molecules could not further adsorb when a layer of PEI had been produced on the silicon surface. As a result, the PEI coating will be a monolayer thick and will not

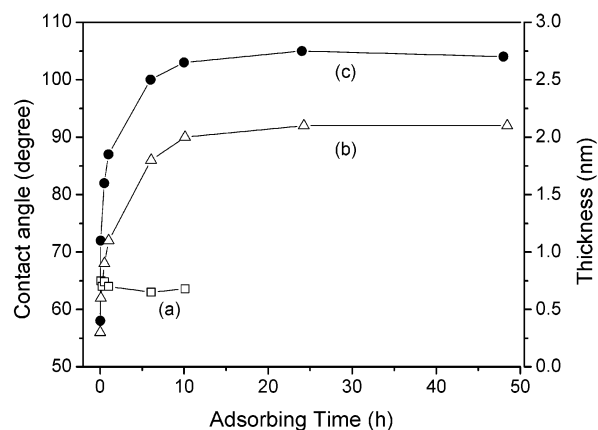


Figure 1. Variations of the thickness and water contact angle of PEI layer on Si substrate and STA-PEI with the immersion duration: (a) thickness of PEI layer versus adsorbing time; (b) thickness of STA layer versus adsorbing time; and (c) contact angle versus STA adsorbing time on PEI surface.

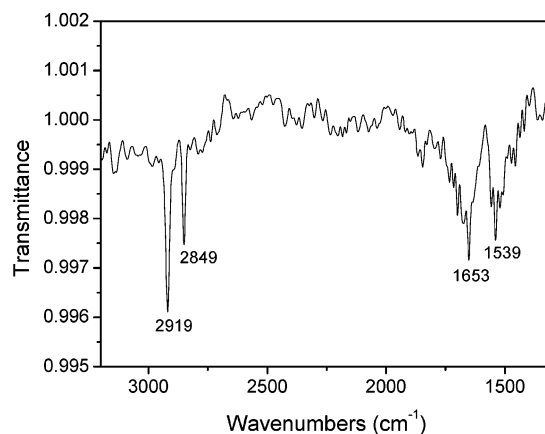


Figure 2. Transmission IR spectrum for STA-PEI film on Si wafer.

become thicker even if the adsorption time is extended to 10 h. Contrary to the above, both the thickness and the contact angle increase with increasing immersion time in STA solution, with the stabilized thickness to be about 2.1 nm and the contact angle to be about 105° at an adsorption duration of 24 h (Figure 1b and c). According to the adsorption kinetics studies, the immersion durations were selected as 15 min and 24 h for the adsorption of PEI and STA, respectively, for samples used in the rest of the study.

The transmission infrared spectrum of the STA film on the PEI-coated Si substrate in the frequency range of 3200–1300 cm^{-1} is shown in Figure 2. Though the baseline is somewhat irregular, it is still observable that the asymmetric [$\nu_{\text{as}}(\text{CH}_2)$] and symmetric [$\nu_{\text{s}}(\text{CH}_2)$] methylene vibration peaks appear at 2919 cm^{-1} and 2849 cm^{-1} , respectively. The peaks at 1650 and 1539 cm^{-1} assigned to amide I ($\nu \text{O}=\text{C}$) and amide II (νNH) indicate that the chemical reaction does take place between the carboxyl group in the STA and the amino groups in the PEI, with the formation of the covalent amide bond.

Figure 3 shows the AFM morphological images of the silicon surface and the STA monolayer film. It can be seen that some holes and grains are observed on the silicon surface (Figure 3a), which might come from the intensive erosion of Piranha solution or the silicon wafer

(56) Hutt, D. A.; Leggett, G. J. *Langmuir* **1997**, *13*, 2740.

(57) Tao, Y. T. *J. Am. Chem. Soc.* **1993**, *115*, 4350.

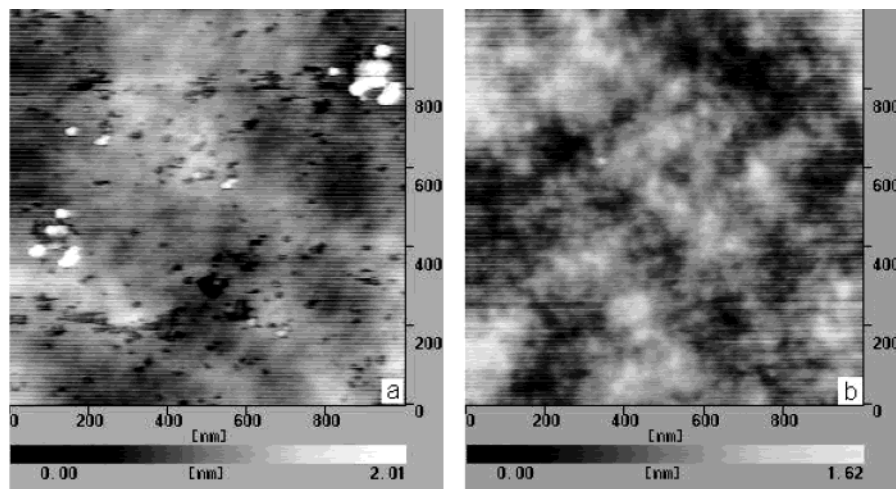


Figure 3. AFM morphologies of the silicon surface (a) and the STA-PEI film thereon (b).

itself. After the generation of the STA-PEI thin film, the surface becomes relatively smooth and homogeneous (Figure 3b), with the root-mean-square (rms) surface roughness to be about 0.26 nm over an area of $2 \mu\text{m} \times 2 \mu\text{m}$ which is a little bit smaller than that of the silicon surface (0.31 nm). Thus, it is rational to conclude that the adsorption of the STA-PEI film helps to improve the quality of the Si wafer surface.

3.2 Microtribological Behavior Characterization. In general, the adhesion force (F_{ad}) between surfaces includes the capillary force (F_{C}) as well as the solid-solid interactions, consisting of van der Waals forces (F_{vdW}), electrostatic forces (F_{E}), and the chemical forces (F_{B}).^{58,59} F_{ad} is expressed as below:

$$F_{\text{ad}} = F_{\text{C}} + F_{\text{vdW}} + F_{\text{E}} + F_{\text{B}}$$

where the capillary force F_{C} closely related to surface wettability is a main contribution to adhesion, while F_{E} is negligible and F_{vdW} has only a small contribution.⁵⁹ As does the term F_{B} , which might play an important role for mated surfaces made of the same or similar materials, such as the Si_3N_4 tip and the SiO_2 surface. In other words, it is possible that the adhesion between Si_3N_4 tip and silicon surface is related to their high pair interaction (a high pair interaction means that the molecules or the atoms are sitting deeply inside their potential⁶⁰). Thus, it is rationally observed that the hydrophilic silicon surface possesses the highest adhesion force of 70.4 nN (Figure 4) due to the high capillary forces and chemical forces between the Si_3N_4 tip and the SiO_2 surface, whereas the STA-PEI thin film has a considerably reduced adhesion force of about 7.1 nN (Figure 4) due to its strong hydrophobicity, which helps to eliminate the capillary force, and due to the negligible chemical force between the STA molecules and the Si_3N_4 tip. It also can be seen from Figure 4 that the PEI coating records a considerably decreased adhesion force of 17.2 nN as compared with that of the silicon surface. This could be attributed to two reasons. First, F_{B} might have a very little contribution to the adhesion in this case because of the large differences in the natures of

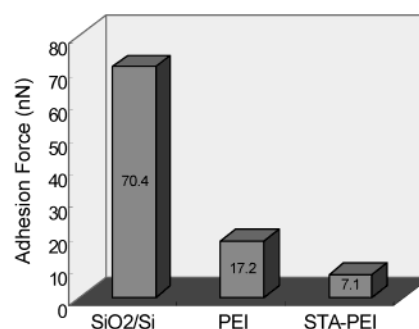


Figure 4. Adhesive forces between an AFM tip and the surfaces of the hydroxylated silicon (SiO_2/Si), PEI surface, and STA-PEI film (RH = 65%).

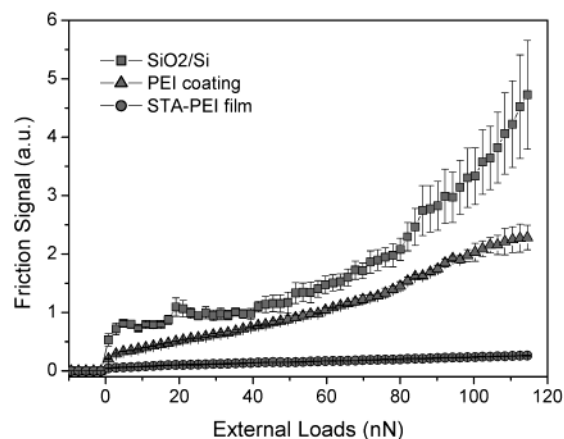


Figure 5. Friction-versus-load curves for the surfaces of the hydroxylated silicon (SiO_2/Si), PEI coating, and STA-PEI film at a scanning velocity of $0.5 \mu\text{m/s}$ (RH = 65%).

the PEI molecules and the Si_3N_4 tip. Second, the amino-terminated PEI surface could easily adsorb organic molecules in air to increase the hydrophobicity during a relatively extended exposure (a few hours) in the adhesive force measurement.

The friction-versus-load curves for the hydroxylated silicon surface, PEI coating, and STA-PEI thin film are plotted in Figure 5. In relating to the adhesion forces shown in Figure 4, it is rational to observe that both films reduce the friction force; the STA-PEI film possesses much better lubricity. Many studies have reported that the friction would decrease with reducing

(58) Binggeli, M.; Mate, C. M. *Appl. Phys. Lett.* **1994**, *65*, 415.

(59) Xiao, X. D.; Qian, L. M. *Langmuir* **2000**, *16*, 8153.

(60) Luengo, G.; Campbell, S. E.; Srdanov, V. I.; Wudl, F.; Israelachvili, J. N. *Chem. Mater.* **1997**, *9*, 1166.

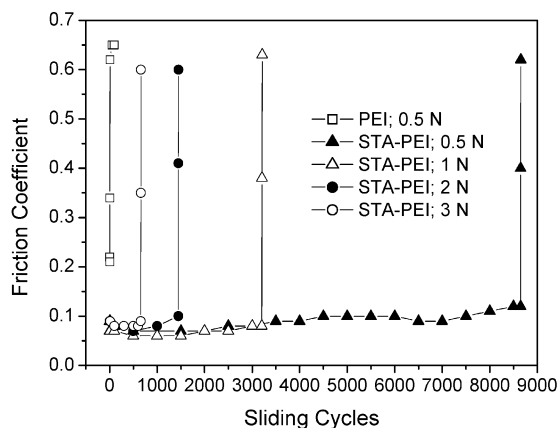


Figure 6. Variation in the friction coefficients with sliding cycles for the PEI coating and STA-PEI film sliding against a Si_3N_4 ball at a sliding velocity of 90 mm/min (RH = 45%).

adhesion on microscope.^{8,19,61} The excellent lubricity of the STA-PEI film is also attributed to the nature of the ordered STA monolayer. In other words, the long-chains of the STA molecules with one end attached to the substrate surface have a significant freedom to swing and rearrange along the sliding direction under shear stress, and therefore yield a smaller resistance. However, the friction force is relatively large for the PEI surface due to its higher adhesion and more severe molecule disordering. Furthermore, the friction force increases faster than the linear extrapolation as the external load exceeds 80 nN, which reflects that wear or displacement of PEI materials occurs. The friction curve for the STA-PEI film is smooth and linear, indicating that the STA-PEI film not only has greatly reduced friction but also possesses good wear resistance. For a Si_4N_3 tip with a radius about 50 nm used in this work, the observed threshold load of 80 nN is roughly estimated to correspond to a Hertzian contact pressure of about 0.9 GPa. It is also seen in Figure 5 that the friction curve for the silicon surface is somewhat irregular and the data are of larger scattering, which implies that wear has occurred between the sample and the AFM tip.

Moreover, a large nonzero friction signal appears at zero external load for the hydroxylated silicon surface, which is attributed to the jump-to-contact instability caused by attractive forces during the approach of the tip to the sample surface. The jump of the tip onto the surface becomes weak for the PEI surface and disappears for the STA-PEI film. Such behaviors are also consistent with the adhesive results (Figure 4); in other words, the jump appears on the strong adhesive surface.

3.3 Macrotribological Behavior Characterization. The macrotribological behaviors of the PEI coating and STA-PEI film are shown in Figure 6. The initial friction coefficient for the PEI surface is about 0.22, but sharply increases to about 0.65, which equals to that of the silicon substrate, after several cycles even under a load as low as about 0.5 N. This indicates that the PEI coating possesses poor load-carrying capacity and wear-resistance, which is consistent with the corresponding microfriction test results. Contrary to the PEI film, the

STA-PEI film shows good friction-reducing behavior and wear-resistance. Namely, it has a friction coefficient of about 0.06–0.09 and antiwear life about 8600 cycles, 3200 cycles, 1400 cycles, and 650 cycles, corresponding to normal loads of 0.5 N, 1 N, 2 N, and 3 N, respectively. The high wear-resistance and load-carrying capacity of the STA-PEI film might be attributed to several factors. First, the PEI macromolecules have densely distributed functional amino groups which are beneficial to the stable attachment of the PEI molecules on the Si substrate. Second, the STA monolayer possesses high elasticity and could endure larger stress, as Houston and his colleagues⁶² reported that the hexadecanetriol SAMs were very compliant at the initial contact by the tip, but became noncompliant as the applied stress continually increased until about 4 GPa. In the non-compliant region, the molecules become trapped between the tip and substrate by the interlocking of nested methylene units, which allows them to virtually elastically support large stress, compression, and shear, without significant lateral displacement, while the initial deformation could be recovered completely after unloading. Third, the hydrogen bonds in the STA-PEI film (see the dashed frame in Scheme 1) between the amide groups could not only stabilize the film but also recover after breaking during the sliding. In other words, although the hydrogen bonds were broken in the presence of the mechanical interaction, they could be recovered and remain to stabilize the film after sliding. In consideration of the energy transformation in the sliding process, the mechanical energy is absorbed and deposited as chemical energy when the hydrogen bonds are broken during the sliding, and then the chemical energy is released as heat energy as the hydrogen bonds are regenerated.

In a previous effort to improve the load-carrying capacity and anti-wear ability of the SAMs, we prepared a self-assembled dual-layer film making use of the chemical adsorption of the STA molecules onto the SAM of 3-(aminopropyl)triethoxysilane (APS).²⁴ The tribological behavior of the resulting dual-layer film was comparatively investigated using the OTS monolayer as a reference. It was found that by introducing hydrogen bonds between the molecules, the STA-APS dual-layer film showed much better friction-reducing and anti-wear ability than the OTS-SAM. It is also noted that the STA-APS film exceeds the STA-PEI film in the number of cycles to failure under different loads. On one hand, the PEI coating combines with the silicon substrate only by physical adsorption, whereas the APS monolayer combines with the substrate by chemical bonds. Furthermore, Si-O-Si bond network exists between the APS molecules, which could contribute to stabilize the STA-APS film. On the other hand, the PEI coating itself has poor wear-resistance and load-carrying capacity (Figures 5 and 6), thus the failure of the STA-PEI film might be originated in the PEI layer. Nevertheless, STA-PEI film shows much better anti-wear ability than the OTS-SAM and PEI films. It offers a good alternative method to improve the tribological properties of a polymer film by chemisorbing long-chain monolayer on the functional polymer surface. In this respect the present work would be meaningful and

(61) Frisbie, C. D.; Rozanyal, L. F.; Noy, A.; Wrighton, M.; Lieber, C. M. *Science*, **1994**, *265*, 2071.

(62) Houston, J. E.; Kim, H. I. *Acc. Chem. Res.* **2002**, *35*, 547.

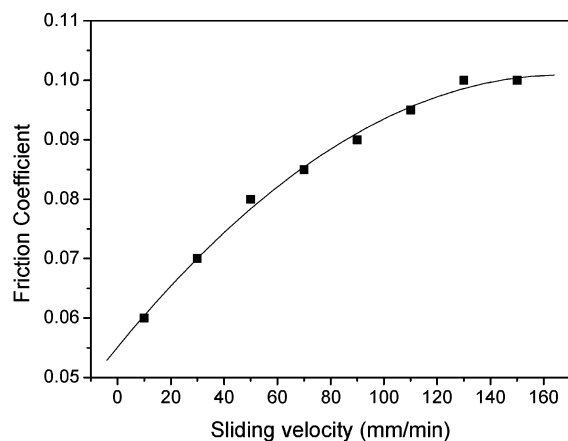


Figure 7. Variation in the friction coefficients with sliding velocities for the STA-PEI film sliding against Si_3N_4 ball at a normal load of 0.5 N.

important for the application of polymer film as a good boundary lubricant.

The effect of sliding velocity on the tribological properties of the STA-PEI film is shown in Figure 7. The friction coefficient increases from 0.06 to 0.10 with increasing sliding velocity and then reaches a plateau at a higher velocity up to 150 mm/min. Such a kind of velocity dependence of the friction was also reported on related microtribological studies of self-assembled films elsewhere,^{15,19,63} which could be reasonably understood by taking into account that the higher shear velocity will intensify the oscillation and distortion of the molecules and then accelerate the dissipation of the accumulated energy.

The SEM morphologies of the worn surfaces of the Si wafer and STA-PEI film after sliding against the Si_3N_4 ball at a normal load of 0.5 N are shown in Figure 8. The worn surface of the Si wafer after only 10 sliding cycles is characterized by severe plastic deformation and fracture (Figure 8a), whereas that of the STA-PEI film at 1000 sliding cycles only shows indistinctive signs of mild scratching (Figure 8b). The above observations of the worn surface morphologies agree well with the corresponding friction and wear behaviors of the STA-PEI film. Namely, different from our previous finding that the OTS monolayer experienced wear at 100 sliding cycles under the same load of 0.5 N,²³ the STA-PEI film possessed much better friction-reducing and anti-wear properties.

4. Conclusion

The self-assembled monolayer of STA in a thickness about 2.1 nm is prepared on a Si wafer coated with a polyethyleneimine (PEI) layer containing amino groups, by way of the formation of a covalent amide bond in the presence of DCCD as the dehydrating reagent. The STA monolayer topped on the hydrophilic PEI layer is highly hydrophobic and has a water contact angle of about

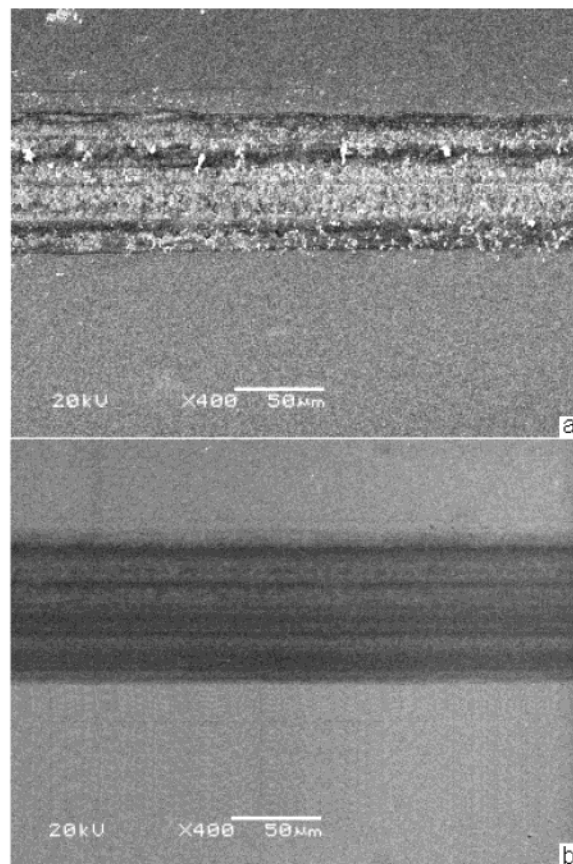


Figure 8. SEM images of the worn surfaces of the substrate and STA-PEI film sliding against a Si_3N_4 ball at a normal load of 0.5 N: (a) bare silicon surface sliding for 10 cycles, and (b) STA-PEI film sliding for 1000 cycles.

105°. The adsorption of the PEI on the Si wafer is completed in a few minutes, whereas at least 24 h is needed for the saturated STA monolayer to form. The PEI coating has relatively high adhesion and friction and poor anti-wear ability, whereas the STA-PEI film possesses good adhesive resistance and high load-carrying capacity and anti-wear ability, which is attributed to the chemical structure of the STA-PEI thin film. The self-assembled dual-layer film of STA-PEI would find promising application in the lubrication and protection of MEMS devices, and it is feasible to improve the tribological properties of polymer film by chemisorbing a long-chain monolayer on the functional polymer surface.

Acknowledgment. We sincerely thank Dr. Xudong Xiao (Department of Physics, Hongkong University of Science and Technology) for his kindness of offering the FFM facility. We also acknowledge the financial support from the National Natural Science Foundation of China (Grants 50375151, 50275142, and 50272068), from 863 project (2002AA302609), and from the Chinese Academy of Sciences (Grant KJCX-SW-L2).

(63) Liu, Y. H.; Wu, T.; Evans, D. F. *Langmuir*, **1994**, *10*, 2241.